Available online at www.sciencedirect.com

ScienceDirect

International Journal of Solids and Structures 45 (2008) 3430–3448

INTERNATIONAL JOURNAL OF SOLIDS AND STRUCTURES

www.elsevier.com/locate/ijsolstr

On the backward Lamb waves near thickness resonances in anisotropic plates

A.L. Shuvalov *, O. Poncelet

Laboratoire de Mécanique Physique UMR CNRS 5469, Université Bordeaux 1, F-33405 Talence Cedex, France

Received 25 August 2007; received in revised form 27 December 2007
Available online 14 February 2008

Abstract

A closed-form expression for the leading-order dispersion coefficient, describing the trend of Lamb-wave branches at their onset from thickness resonances, is derived for an arbitrary anisotropic plate. The sign of this coefficient and hence of the in-plane group velocity near cutoffs decides the existence or non-existence of the backward Lamb waves without a necessity to calculate the dispersion branches. A link between the near-cutoff dispersion of Lamb waves and the curvature of bulk-wave slowness curves in a sagittal plane is analyzed. It is established that a locally concave slowness curve of a bulk mode entails the backward Lamb waves at the onset of branches emerging from this bulk mode resonances of high enough order. A simple sufficient condition for no backward Lamb waves near the resonances associated with a convex slowness curve is also noted. Two special cases are discussed: the first involves the coupled resonances of degenerate bulk waves, and the second concerns quasi-degenerate resonances which give rise to pairs of dispersion branches with a quasilinear positive and negative onset. Occasions of the backward Lamb waves in isotropic plate materials are tabulated.

Keywords: Anisotropic plate; Thickness resonance; Backward Lamb waves; Negative group velocity

1. Introduction

One of the remarkable properties of guided waves in a free plate (Lamb waves) is the possibility of their so-called backward propagation. This phenomenon first came to light about half a century ago (Mindlin, 1955, 1960; Tolstoy and Usdin, 1957), when it was found that Lamb waves in isotropic plates can have the phase front and the averaged energy flux travelling in exactly opposite directions along a plate, in which sense the group velocity is negative (with respect to the positive phase velocity). As shown by Mindlin (1955, 1960) and mentioned thereafter in many textbooks, the backward propagation in isotropic plates is typically confined to the onset of the first symmetric and, more rarely, of the first antisymmetric dispersion branches. For anisotropic plates, the wave vector (orthogonal to the phase front) and the group-velocity vector (equal to the energy velocity, see Auld, 1973) may be not parallel, in which case a backward propagation implies that

* Corresponding author.
E-mail address: a.shuvalov@lmp.u-bordeaux1.fr (A.L. Shuvalov), .

0020-7683/$ - see front matter © 2008 Elsevier Ltd. All rights reserved.
doi:10.1016/j.ijsolstr.2008.02.004

these two vectors in the boundary plane have a negative projection on each other. Already early systematic numerical modelling of Lamb waves in anisotropic plates (e.g., Solie and Auld, 1973; Li and Thompson, 1990) has revealed numerous examples of the ranges of negative in-plane group velocity occurring at the onsets of different dispersion branches. Identifying these branches in a way which would be less effort-consuming than numerical computing of the whole dispersion spectrum is of practical interest in view of particular significance of the backward Lamb waves for various evaluation and imaging techniques (Liu et al., 2000; Germano et al., 2002; Durinck et al., 2002; Parygin et al., 2000; Marston, 2003; Holland and Chimenti, 2004; Clorennec et al., 2006, 2007; Balogun et al., 2007). They also bear important implications for numerical schemes involving the normal-mode decomposition and perfectly matched layers (Pagneux and Maurel, 2002; Castaings and Hosten, 2003; Skelton et al., 2007). The backward Lamb waves play a pivotal role for some other wave-guiding phenomena, e.g., they are intimately related to the mode trapping in curved waveguides (Gridin et al., 2005; Kaplunov et al., 2005; Postnova and Craster, 2007). Note also interesting observations which have been made by Pichugin and Rogerson (2001, 2002) for the backward guided waves in pre-stressed incompressible plates.

It is clear that the backward Lamb waves are most likely to occur along the onsets of (non-fundamental) dispersion branches. The group velocity is zero at their cutoffs corresponding to the thickness resonances,[1] and it may, generally speaking, turn either positive or negative near the cutoffs, which is seen as, respectively, upward or downward bent of the frequency versus horizontal wave vector dispersion branches $\omega_n(k)$. In order to identify which is the case, it suffices to find the coefficient of leading-order (quadratic) dispersion $\omega_n(k) - \omega_n(0) \sim O(k^2)$ near the cutoffs and to inspect its sign. A negative sign indicates the backward propagation. A near-cutoff dispersion coefficient in an anisotropic plate has been derived for a fixed propagation direction parallel to the twofold symmetry axis by Kaul and Mindlin (1962a,b), and, more recently, for an arbitrary propagation direction along the plate boundary containing the axis of transverse isotropy by Kaplunov et al. (2000). An investigation of the sign of this coefficient has been beyond the scope of those studies; however, it is noteworthy that its explicit representation by Kaul and Mindlin (1962a,b) involves the curvature of the slowness curve of the resonant bulk wave. Such a link may be expected to pertain to any anisotropy of the problem, and if so, it suggests to hinge the sign analysis of the near-cutoff dispersion on the local shape of the bulk-wave slowness surface.

The present paper tackles the problem in the general case, which implies unrestricted anisotropy of plate material and arbitrary propagation direction in it. This means dealing with a dispersion equation, which does not split into two independent ones for symmetric and antisymmetric Lamb waves (as it does for the cases treated in by Kaul and Mindlin (1962a,b) and Kaplunov et al. (2000)). The problem is set up in Section 2. Applying the perturbation theory for 'long waves with high frequency' (k is small, ω is not) yields the leading-order dispersion coefficient near thickness resonances, see Section 3. For a typical situation involving a single resonant bulk wave, this coefficient can be presented as a sum of two terms: one of them describes a local shape of slowness curve of the resonant bulk wave in the sagittal-plane cut and has the sign of its curvature, while the other term accounts for the interference of the resonant wave with other partial modes constituting the Lamb-wave packet in the resonance vicinity. The ratio of the latter to former is, among other factors, inversely proportional to the dispersion-branch number n. Hence a concave shape of the bulk-wave slowness curve may be expected to further the occurrence of backward Lamb waves at the onset of branches of large enough number n (high-order branches). This is analyzed in detail in Section 4. A somewhat particular case concerning degenerate resonances of transverse waves in a plate with the faces orthogonal to the fourfold or threefold symmetry axis is treated in Section 5. The point is that, so far as the sagittal plane is not parallel to the symmetry plane, there is a strong coupling between two quasi-degenerate bulk modes composing the Lamb-wave packet near a degenerate resonance. In consequence, the leading-order dispersion coefficient for these branches is no longer as simple as a linear superposition of two terms related, respectively, to the bulk-wave slowness curve and to the interference. However, an asymptotic form of the coefficient for high-order branches restores such an additive structure, and it is still the curvature of the bulk-wave slowness curve which essentially determines the sign of dispersion once the branch number n is large enough. Another special

[1] Throughout the paper, the cutoffs and thickness resonances are understood as corresponding to the normal incidence only.

case, considered in Section 6, is prompted by the observation of Mindlin (1955, 1960) and Kaul and Mindlin (1962a,b) that a theoretical possibility of bulk-wave velocity ratio which is exactly equal to a rational fraction enables a succession of degenerate resonances such that produce branches with a linear (rather than quadratic) leading-order dispersion $\omega_n(k)$ at the onset. Certainly the above equality can never be precisely the case for real materials. At the same time, an occasional proximity of two resonances associated with different bulk waves is a fairly common event. It is demonstrated that a sequence of pairs of closely situated resonances under certain conditions gives rise to pairs of dispersion branches with quasilinear positive and negative onsets, the latter corresponding to the backward Lamb waves. In this case, their occurrence on the high-order branches is independent of the shape of resonant bulk-wave slowness curve. The concluding section (Section 7) briefly touches the existence of backward Lamb waves across the dispersion spectrum.

2. Background

Consider an infinite plate of thickness d made from a homogeneous non-viscous anisotropic material with the density ρ and the stiffness tensor c_{ijkl}. The plate is assumed free of traction (see however Eq. (10) below). Let $\mathbf{n}$ be a unit normal to the boundary plane. Each of three pairs of up- and downgoing bulk waves, propagating with the phase velocity c_α ($\alpha = 1,2,3$) along $\mathbf{n}$, produces a sequence of thickness resonances with the frequency

$$\Omega_{n,\alpha} = \frac{\pi n c_\alpha}{d}, \quad n = 1,2,\ldots, \tag{1}$$

where n enumerates both the resonances associated with a given αth bulk mode and the dispersion branches originating at these resonances. A deviation from the normal incidence causes coupling with the other bulk modes into a Lamb-wave packet with the frequency $\omega_{n,\alpha}(\mathbf{k})$ depending on the horizontal wave vector $\mathbf{k} = k\mathbf{m}$, where

$$\mathbf{m}(\theta) = \mathbf{e}_1 \cos\theta + \mathbf{e}_2 \sin\theta \tag{2}$$

is a unit vector indicating the propagation direction orthogonal to $\mathbf{n}$. The polar angle θ parametrizes a bundle of sagittal planes ($\mathbf{m}$,$\mathbf{n}$) spanned by given $\mathbf{n}$ and various vectors $\mathbf{m}(\theta)$ orthogonal to $\mathbf{n}$. An orthogonal triad of reference vectors $\mathbf{e}_1$, $\mathbf{e}_2$, $\mathbf{n}$ may generally have an arbitrary orientation with respect to the crystallographic coordinate system X_1, X_2, X_3. For a fixed orientation θ of the sagittal plane ($\mathbf{m},\mathbf{n}$), the cutoffs $\Omega_{n,\alpha}$ give rise to (non-fundamental) dispersion branches $\omega_{n,\alpha}(k)$. In the cutoff vicinity, they expand in even powers of $|kd| \ll 1$ (unless a theoretically possible exception discussed in Section 6), so that

$$\omega_{n,\alpha}(k,\theta) = \Omega_{n,\alpha} + \frac{c_\alpha W_{n,\alpha}(\theta)}{2\pi n d}(kd)^2 + \boldsymbol{O}[(kd)^4], \quad W_{n,\alpha}(\theta) = \frac{\pi n}{c_\alpha d}\left[\frac{\partial^2 \omega_{n,\alpha}(k,\theta)}{\partial k^2}\right]_{k=0}, \tag{3}$$

where $W_{n,\alpha}(\theta)$ is a dimensionless coefficient to be found. It will be referred to as the (leading-order) dispersion coefficient in tacit understanding that a common factor $\sim n^{-1}$ is extracted from its definition (3), which is done for the convenience of the forthcoming discussion and graphical display. In the present context k is real, and the group velocity $\mathbf{g}_{n,\alpha}$ of Lamb waves near the cutoffs writes out as

$$\mathbf{g}_{n,\alpha}(k,\theta) = \frac{c_\alpha k d}{\pi n}\left[W_{n,\alpha}(\theta)\mathbf{m} + \frac{1}{2}\frac{\mathrm{d}W_{n,\alpha}(\theta)}{\mathrm{d}\theta}\mathbf{t}\right] + \boldsymbol{O}[(kd)^3] \equiv g^{(\mathbf{m})}_{n,\alpha}\mathbf{m} + g^{(\mathbf{t})}_{n,\alpha}\mathbf{t}, \tag{4}$$

where $\mathbf{t} = \mathbf{m} \times \mathbf{n}$. Thus, if $W_{n,\alpha}(\theta) < 0$ then the onset of the branch $\omega_{n,\alpha}(k,\theta)$, emerging for a given θ from the cutoff $\Omega_{n,\alpha}$, bends downwards and yields the backward propagating Lamb waves with a negative in-plane group velocity $g^{(\mathbf{m})}_{n,\alpha}$. Its out-of-plane component $g^{(\mathbf{t})}_{n,\alpha}$ in anisotropic plates is generally non-zero, except for ($\mathbf{m},\mathbf{n}$) being a symmetry plane and probably for some other secluded orientations of $\mathbf{m}(\theta)$. Introduce a few notations for the future use. Let $\mathbf{a}_\alpha$ be the unit mutually orthogonal polarization vectors of the bulk modes travelling along $\mathbf{n}$ with the velocities c_α. These are defined by the Christoffel equation

$$n_j c_{ijkl} n_k a_{\alpha l} = \rho c_\alpha^2 a_{\alpha i}, \quad \alpha = 1,2,3. \tag{5}$$

Where appropriate, the index α will be specialized as $\alpha = L$ for the longitudinal wave and $\alpha = SV$, SH for the pure transverse in-plane and out-of-plane waves, respectively; side by side with the above, we shall also use $\alpha = T$ for the degenerate transverse waves and $\alpha = T1$, $T2$ for the slow and fast quasi waves, respectively. It is noted that the same transverse polarization $\mathbf{a}_\alpha$, which is fixed for a fixed $\mathbf{n}$, is ascribed as quasi-transverse or pure (in-plane or out-of-plane) transverse relatively to the sagittal plane $(\mathbf{m},\mathbf{n})$ with running orientation θ. A contraction of the tensor c_{ijkl}/ρ with the polarization vectors $\mathbf{a}_{1,2,3}$ and the reference vectors $\mathbf{n}$, $\mathbf{m}(\theta)$ is denoted as follows:

$$\|\mathbf{mm}\|_{\alpha\beta} = \frac{1}{\rho} a_{\alpha i} m_j c_{ijkl} m_k a_{\beta l}, \quad \|\mathbf{mn}\|_{\alpha\beta} = \frac{1}{\rho} a_{\alpha i} m_j c_{ijkl} n_k a_{\beta l} (= \|\mathbf{nm}\|_{\beta\alpha}), \qquad \alpha, \beta = 1, 2, 3. \tag{6}$$

In these terms, for instance, $c_\alpha^2 = \|\mathbf{nn}\|_{\alpha\alpha}$. Inserting (2) visualizes a dependence of $\|\mathbf{mm}\|_{\alpha\beta}$, $\|\mathbf{mn}\|_{\alpha\beta}$ on the orientation θ of $\mathbf{m}(\theta)$.

3. Dispersion coefficient near an uncoupled resonance

3.1. Arbitrary anisotropy

Let the normal to the plate boundary $\mathbf{n}$ and the Lamb-wave propagation direction $\mathbf{m}(\theta)$ have a generic orientation with respect to the symmetry elements (if there are any) of the plate stiffness tensor c_{ijkl} of arbitrary anisotropy. Consider the vicinity of nth thickness resonance of some αth bulk wave. For the moment, the given resonance is assumed non-degenerate, i.e. its frequency $\Omega_{n,\alpha}$ is such that $\Omega_{n,\alpha} \neq \Omega_{m,\beta}$ for any m,β other than n,α (otherwise see a remark on SH-decoupling in Section 3.2 and also Sections 5 and 6). Omitting the details of a rather tedious but straightforward derivation, the near-cutoff dispersion coefficient $W_{n,\alpha}(\theta)$ introduced in Eqs. (3) can be obtained in a closed form as a sum of two terms:

$$W_{n,\alpha}(\theta) = W_\alpha^{(1)}(\theta) + W_{n,\alpha}^{(2)}(\theta), \quad \alpha = 1, 2, 3;\ n = 1, 2, \ldots \tag{7}$$

The first term is

$$W_\alpha^{(1)}(\theta) = \frac{1}{c_\alpha^2}\left[\|\mathbf{mm}\|_{\alpha\alpha} - \frac{(\|\mathbf{mn}\|_{\alpha\alpha})^2}{c_\alpha^2} + \sum_{\beta=1,\beta\neq\alpha}^{3} \frac{(\|\mathbf{mn}\|_{\alpha\beta} + \|\mathbf{mn}\|_{\beta\alpha})^2}{c_\alpha^2 - c_\beta^2}\right] = \frac{c_\alpha \kappa_\alpha(\theta)}{\cos^3\psi_\alpha(\theta)}. \tag{8}$$

The latter equality shows that this term is entirely determined by the local geometrical parameters of the bulk-wave slowness curve $S_\alpha(\theta)$ in the cut by the sagittal plane $(\mathbf{m},\mathbf{n})$. Apart from the bulk-wave slowness $s_\alpha = 1/c_\alpha$ itself, these parameters are the curvature κ_α of S_α and the angle ψ_α between the plate normal $\mathbf{n}$ and the normal $\mathbf{N}_\alpha$ to S_α. Both $\kappa_\alpha(\theta)$ and $\mathbf{N}_\alpha(\theta)$ are taken at the point $\mathbf{s}_\alpha = s_\alpha \mathbf{n}$. The normal to S_α is parallel to the $(\mathbf{m},\mathbf{n})$-projection of the group velocity $\mathbf{V}_\alpha$ of the αth bulk wave travelling along $\mathbf{n}$, i.e. $\mathbf{N}_\alpha \| \ (\mathbf{m}\times\mathbf{n})\times\mathbf{V}_\alpha \times(\mathbf{m}\times\mathbf{n})$, whence $\cos\psi_\alpha = [1 + (\|\mathbf{mn}\|_{\alpha\alpha})^2/c_\alpha^4]^{-1/2} (> 0)$. Deviation from the normal incidence causes a slight non-alignment of the group-velocity vectors $\mathbf{V}_\alpha$ of up- and downgoing bulk modes of the αth branch, and a non-zero resultant of $\mathbf{m}$-components of $\mathbf{V}_\alpha$ contributes to the in-plane group velocity $g_{n,\alpha}^{(\mathbf{m})}$ of Lamb waves (see Eq. (4)). This contribution is precisely what is described by the term $W_\alpha^{(1)}(\theta)$. Recalling that the slowness curve S_α is invariant with respect to the inversion centre, it is evident why the sign of $W_\alpha^{(1)}$ is prescribed by the sign of the curvature κ_α of S_α. This is illustrated by Fig. 1.

The second term is

$$W_{n,\alpha}^{(2)}(\theta) = \frac{4}{\pi n} \sum_{\beta=1,\beta\neq\alpha}^{3} \frac{(c_\alpha^2\|\mathbf{mn}\|_{\alpha\beta} + c_\beta^2\|\mathbf{mn}\|_{\beta\alpha})^2}{c_\alpha^3 c_\beta (c_\alpha^2 - c_\beta^2)^2} \tan\left[\frac{\pi n}{2}\left(1 - \frac{c_\alpha}{c_\beta}\right)\right]. \tag{9}$$

It describes interference of the modes of αth (resonant) bulk-wave branch with the modes of two other branches $\beta \neq \alpha$ incorporated into the Lamb-wave packet near the resonance. The interference fall-off with growing resonant frequency leads to inverse proportionality of this term to the number n of the dispersion branch $\omega_{n,\alpha}(k)$.

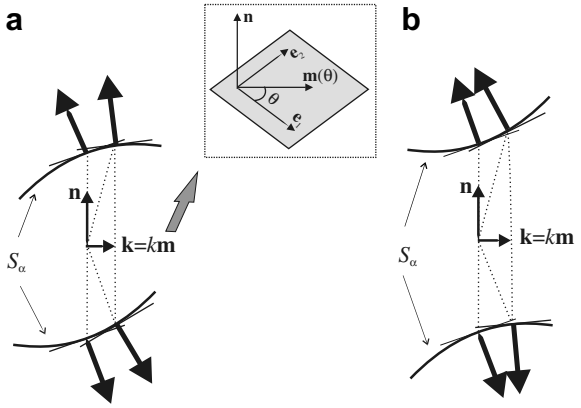

Fig. 1. A fragment of the bulk-wave slowness curve S_α in the cut by the sagittal plane $(\mathbf{m},\mathbf{n})$, which is (a) convex and (b) concave around the reference point $\mathbf{s}_\alpha = s_\alpha\,\mathbf{n}$. The bold vectors are normals to S_α which are parallel to the projections on $(\mathbf{m},\mathbf{n})$ of the group velocity $\mathbf{V}_\alpha$ of the up- and downgoing bulk modes propagating along $\mathbf{n}$ and in the close vicinity. The inserted box shows the geometry of the problem.

Note in passing that Eq. (7) remains valid for a plate which is clamped (has zero displacement) on both faces or is clamped on one face and free on the other, except some modifications in the interference term. For example, this term for a clamped plate is as follows:

$$[W^{(2)}_{n,\alpha}(\theta)]_{\text{clamped}} = \frac{4}{\pi n}\sum_{\beta=1,\beta\neq\alpha}^{3}\frac{c_\beta}{c_\alpha}\left(\frac{\|\mathbf{mn}\|_{\alpha\beta}+\|\mathbf{mn}\|_{\beta\alpha}}{c_\alpha^2-c_\beta^2}\right)^2\tan\left[\frac{\pi n}{2}\left(1-\frac{c_\alpha}{c_\beta}\right)\right]. \tag{10}$$

Also note that Eq. (3) with (7)–(10) applies for either sign of $(kd)^2$, i.e. for both real and imaginary k.

3.2. Explicit simplifications due to material symmetry

Eqs. (7)–(9) reduce their explicit form when at least one of the three reference planes (the sagittal plane $(\mathbf{m},\mathbf{n})$, the boundary plane orthogonal to $\mathbf{n}$, and the plane orthogonal to $\mathbf{m}$) is a symmetry plane. Then the interference between certain bulk modes $\alpha,\beta = 1,2,3$ turns to zero. Let us list these cases and outline the resulting simplifications.

If, for a given $\mathbf{n}$, the orientation of $\mathbf{m}$ is fixed so that the sagittal plane $(\mathbf{m},\mathbf{n})$ is a symmetry plane of the tensor c_{ijkl}, then the identity

$$\|\mathbf{mn}\|_{\alpha\beta} = \|\mathbf{mn}\|_{\beta\alpha} = 0 \tag{11}$$

holds when either α or β corresponds to the shear horizontal (SH) bulk mode travelling along $\mathbf{n}$ with the out-of-plane polarization parallel to $\mathbf{t} = \mathbf{m}\times\mathbf{n}$. The SH waves in a plate are also uncoupled from the in-plane Lamb waves (Auld, 1973), and their dispersion branches are defined explicitly by the well-known relation

$$\omega^2_{n,SH}(k) = c^{(\mathbf{n})2}_{SH}\left(\frac{\pi n}{d}\right)^2 + c^{(\mathbf{m})2}_{SH}k^2, \tag{12}$$

where $c^{(\mathbf{n})}_{SH}$ is the velocity of SH bulk mode travelling along $\mathbf{n}$, and $c^{(\mathbf{m})}_{SH}$ is the velocity of SH bulk mode carrying energy along $\mathbf{m}$. As a trivial test of Eqs. (7)–(9), their applying to the $\alpha = SH$ family of plate branches verifies the leading-order coefficient $W_{n,SH} = c^{(\mathbf{m})2}_{SH}/c^{(\mathbf{n})2}_{SH} > 0$, following from (12) at $kd \ll 1$. For the in-plane Lamb waves, the sums in Eqs. (8) and (9) reduce due to (11) to a single term each. Recall that Eqs. (7)–(9) have been restricted to a non-degenerate resonant bulk wave with the velocity $c_\alpha \neq c_\beta$ along $\mathbf{n}$. Attention is drawn to the fact that this restriction is certainly lifted in the case of a symmetric sagittal plane $(\mathbf{m},\mathbf{n})$. Indeed if the normal $\mathbf{n}$ is a direction of degeneracy $c_\alpha = c_\beta$ (an acoustic axis) such that lies in a symmetry plane, then one of the degenerate waves is the SH mode (a degeneracy between the L and SV waves is a purely theoretical possibility) and hence its resonances give rise to the SH plate waves, which are uncoupled from the in-plane Lamb waves regardless of degeneracy.

If $\mathbf{m}$ is a fixed direction orthogonal to a symmetry plane, then Eq. (11) holds for the αth and βth bulk modes polarized in this symmetry plane so that $\mathbf{a}_\alpha \cdot \mathbf{m} = \mathbf{a}_\beta \cdot \mathbf{m} = 0$. The sums in (8) and (9) for the cutoffs, associated with either of these two bulk modes, reduce to a single term leading to the result of Kaul and Mindlin (1962a,b). Also, $\|\mathbf{mn}\|_{\alpha\alpha} = 0$ for any $\alpha = 1,2,3$.

If the plate boundary is a symmetry plane and $\mathbf{m}(\theta)$ has an arbitrary orientation in it, then again Eq. (11) holds for the αth and βth bulk modes polarized in this symmetry plane, i.e. when $\mathbf{a}_\alpha \cdot \mathbf{n} = \mathbf{a}_\beta \cdot \mathbf{n} = 0$. Also, $\|\mathbf{mn}\|_{\alpha\alpha} = 0$ for $\alpha = 1,2,3$ and $\|\mathbf{mn}\|_{\alpha\beta} = c_\alpha^2 \mathbf{m} \cdot \mathbf{a}_\beta$ for $\mathbf{a}_\alpha \| \mathbf{n}$. Plugging this into Eqs. (7)–(9) and assuming in addition that the plate has a transversely isotropic axis in the boundary plane leads to the result of Kaplunov et al., 2000.

For the future discussion, it is useful to exemplify the coefficient $W_{n,\alpha}(\theta)$ for an orthorhombic plate with all three reference planes being the symmetry planes. Let the coordinate axes be orthogonal to the symmetry planes and specify them as $X_{1,2} \| \mathbf{e}_{1,2}$, $X_3 \| \mathbf{n}$. The index α of the bulk waves travelling along $\mathbf{n}$ is specialized according to their polarizations as $\alpha = L, SV, SH$, see Section 2. By (7)–(9), the leading-order dispersion coefficients $W_{n,\alpha}(\theta)$ for $\theta = 0$ ($\mathbf{m} = \mathbf{e}_1$, $\mathbf{t} = \mathbf{e}_2$) are

$$
\begin{aligned}
W_{n,SH}(0) &= \frac{c_{66}}{c_{44}},\\
W_{n,SV}(0) &= \frac{c_{11}(c_{33}-c_{55}) - (c_{13}+c_{55})^2}{c_{55}(c_{33}-c_{55})} + \frac{4}{\pi n}\sqrt{\frac{c_{55}}{c_{33}}}\left(\frac{c_{13}+c_{33}}{c_{33}-c_{55}}\right)^2 \tan\left[\frac{\pi n}{2}\left(1-\frac{c_{SV}}{c_L}\right)\right],\\
W_{n,L}(0) &= \frac{c_{33}c_{55} + c_{13}^2 + 2c_{13}c_{55}}{c_{33}(c_{33}-c_{55})} + \frac{4}{\pi n}\left(\frac{c_{55}}{c_{33}}\right)^{3/2}\left(\frac{c_{13}+c_{33}}{c_{33}-c_{55}}\right)^2 \tan\left[\frac{\pi n}{2}\left(1-\frac{c_L}{c_{SV}}\right)\right],
\end{aligned}
\tag{13}
$$

where $c_L = \sqrt{c_{33}/\rho}$ and $c_{SV} = \sqrt{c_{55}/\rho}$. Obviously the coefficients $W_{n,\alpha}$ for $\theta = 90°$ follow from (13) on interchanging the indices 1, 2 in c_{ijkl}. Eq. (13) has been used by Shuvalov et al. (2006) for analyzing a link between the backward Lamb waves in a free plate and the leaky waves in this plate loaded by fluid.

It is clear that Eq. (13) with $c_{13} = c_{23}$, $c_{44} = c_{55}$ describes the near-cutoff dispersion coefficient $W_{n,\alpha}$ in any sagittal plane if the plate normal $\mathbf{n}$ is parallel to the axis of transverse isotropy. Interestingly, if $\mathbf{n}$ is parallel to the threefold or fourfold symmetry axis, then the coefficient $W_{n,L}$ is also angular independent and is given by Eq. $(13)_3$ for any θ. For an isotropic plate, Eq. (13) reduces to a trivial equality $W_{n,SH} = 1$ and to the well-known Mindlin's (1955, 1960) result for the in-plane Lamb branches:

$$
\begin{aligned}
W_{n,SV} &= 1 + \frac{16}{\pi n}\frac{c_T}{c_L}\tan\left[\frac{\pi n}{2}\left(1-\frac{c_T}{c_L}\right)\right],\\
W_{n,L} &= 1 + \frac{16}{\pi n}\frac{c_T^3}{c_L^3}\tan\left[\frac{\pi n}{2}\left(1-\frac{c_L}{c_T}\right)\right].
\end{aligned}
\tag{14}
$$

It is noteworthy that for both isotropic and transversely isotropic cases the coefficients $W_{n,\alpha}$ near the degenerate transverse resonances do follow from Eq. (13) which has been obtained for a fixed symmetric sagittal plane, but they cannot be obtained by a direct substitution of appropriate c_{ijkl} into the initial formulas (7)–(9). This is because the case of degeneracy in the absence of SH/in-plane uncoupling is not described by (7)–(9) and must be treated in a special way, see Section 5.

3.3. A digression on the case of isotropy

It is evident that testing the sign of the coefficients given by the Mindlin's formulas (14) enables one to tabulate the occasions of backward Lamb waves near cutoffs as a function of c_T/c_L, i.e. for all the variety of isotropic materials. We could not, however, find such data published, so we present it in Fig. 2. It is arranged in the form of two 2D diagrams identifying the dispersion trend at the onset of the in-plane antisymmetric and symmetric families of branches A_n and S_n in any isotropic plate ($0 < c_T/c_L < \sqrt{3}/2$). The computation is based on Eq. (14) complemented by the conversion rule into symmetric/antisymmetric output, which implies successive picking the A_n cutoffs from the least among the odd numbered transverse-wave cutoffs and the even numbered longitudinal-wave cutoffs, and the inverse for picking S_n. It is hoped that this simple chart may be useful

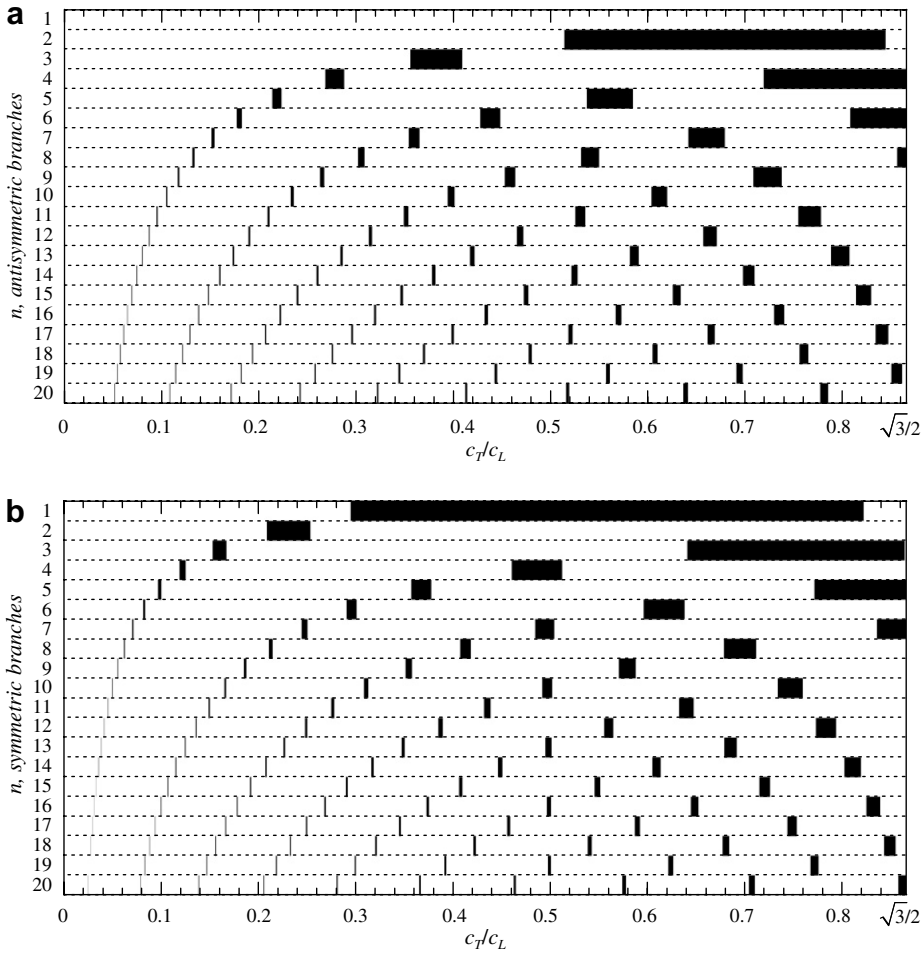

Fig. 2. Occurrence of the forward (blank zones) and backward (black zones) Lamb waves at the onsets of (a) the antisymmetric branches A_n and (b) the symmetric branches S_n in isotropic plates.

for practical use. For instance, it is seen that the first symmetric branch S_1 emerges with a positive group velocity if $c_T/c_L < \tau_1 \approx 0.295$ or $c_T/c_L > \tau_2 \approx 0.822$, where τ_1 and τ_2 satisfy the equations $8\tau\tan(\pi\tau) = \pi$ and $16\tau^3\cot(\pi/2\tau) = -\pi$, respectively. This possibility has been overlooked by Werby and Überall (2002). Note that the narrow zones of negative dispersion, which arise near rational values of c_T/c_L, are inevitability missing in a graphical display when they are narrower than a finite step between sampling points (10^4 points have been used for computing Fig. 2). The origin of these zones is discussed in Section 6.

4. Discussion and numerical examples

4.1. Backward Lamb waves and a local shape of bulk-wave slowness curve

We now get back to the general form of Eqs. (7)–(9) and proceed to the sign analysis of the coefficient $W_{n,\alpha} = W^{(1)}_{\alpha} + W^{(2)}_{n,\alpha}$ of the leading-order dispersion defined by Eq. (3) (note a common factor $\sim n^{-1}$ therein). The first term $W^{(1)}_{\alpha}$ is independent from the branch number n, while the second term $W^{(2)}_{n,\alpha}$ is inversely proportional to n. Therefore, once n becomes large enough, the sign of $W_{n,\alpha}$ shall be determined as a rule by the sign of $W^{(1)}_{\alpha}$, i.e. merely by the sign of curvature κ_α of the bulk-wave slowness curve S_α for the αth resonant wave. In other words, a local concavity of S_α in a sector embracing the direction of the plate normal $\mathbf{n}$ promotes the

existence of backward Lamb waves at the onset of dispersion branches emerging from high-frequency resonances of the αth bulk wave. There are two basic points in question. First is how large the branch number n must be in order to cause a dominance of $W_{\alpha}^{(1)}$ over $W_{n,\alpha}^{(2)}$ (whose decreasing rate $W_{n,\alpha}^{(2)} \sim n^{-1}$ is not actually that fast). Secondly, in view of a 'tricky' tangent factor in $W_{n,\alpha}^{(2)}$, it is pertinent to inquire how persistent the prevalence of $W_{\alpha}^{(1)}$ over $W_{n,\alpha}^{(2)}$ is going to be with further growing n.

In order to fix ideas, consider an example of the rutile (TiO_2) plate with the normal **n** parallel to the [100]-crystallographic axis. The material constants of TiO_2 are taken from Auld (1973), and the DISPERSE package (Pavlakovic et al., 1997) has been employed in the following for computing exact dispersion curves. Application of Eq. (3) with (7)–(9) to approximating the near-cutoff dispersion for a non-symmetric orientation of the sagittal plane is demonstrated in Fig. 3. First we note in passing a markedly flat onset of the dispersion branches $\omega_{n,T1}(k)$ starting from the resonances of the $\alpha = T1$ quasi-transverse wave whose slowness surface S_{T1} has small curvature κ_{T1} at the reference point (see the inset). Let us now look specifically at the family of branches $\omega_{n,T2}(k)$ emerging from the resonances of the $\alpha = T2$ wave with a locally concave slowness curve S_{T2}. In Fig. 3, the first few of these branches ($n = 1, \ldots, 6$) bend upwards, while the higher-order ones

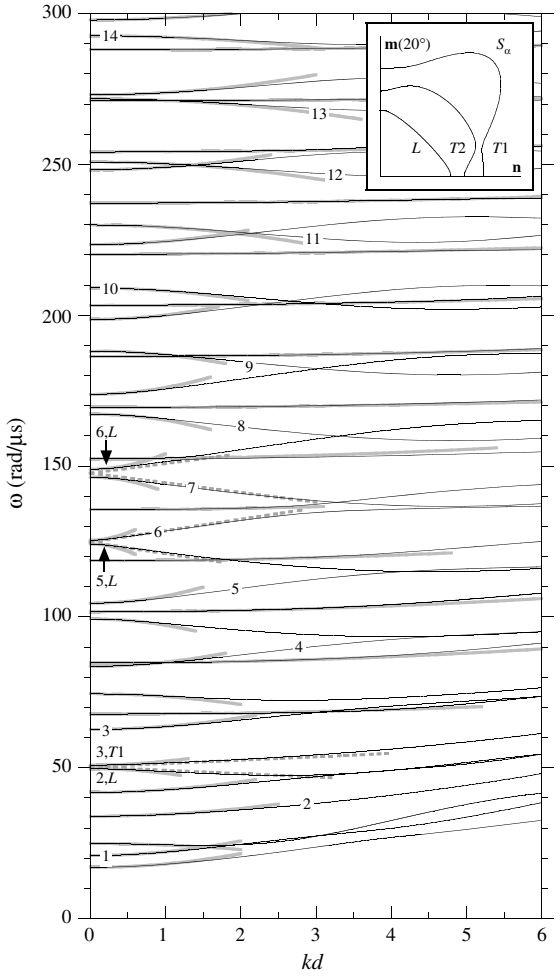

Fig. 3. The onset of non-fundamental dispersion branches $\omega_{n,\alpha}(k)$ in the (100)-cut TiO_2 plate for the sagittal plane (**m**, **n**) making the angle $\theta = 20°$ with the principal crystallographic axis [001]. Solid lines are exact curves (the scale preclude resolving some branch-crossing/repulsion occasions), gray lines show their leading-order (quadratic) approximation. The inset displays the bulk-wave slowness curves S_α in the sagittal plane (within the symmetry-irreducible sector). The numbers $n = 1, \ldots, 14$ are ascribed to the branches $\omega_{n,T2}(k)$ starting at the resonances of the $\alpha = T2$ bulk wave, whose slowness curve is concave around **n**. In addition, the linear approximation (see Section 6.2) is shown by dashed lines for the several branches with closely situated cutoffs.

($n = 7, \ldots 14$) bend downwards and hence correspond to the backward Lamb waves. To verify a systematic link between the near-cutoff dispersion and the local shape of the bulk-wave slowness curve, Fig. 4 presents the dispersion coefficients $W_{n,T2}(\theta)$ given by Eqs. (7)–(9) for the $\alpha = T2$ family of branches as a function of running orientation θ of the sagittal plane $(\mathbf{m}, \mathbf{n})$ in the (100)-cut TiO_2 plate ($\theta = 20°$ corresponds to the setting of Fig. 3). The slowness curve $S_{T2}(\theta)$ in a cut by the sagittal plane is concave for $\theta < \theta_0$ and convex for $\theta > \theta_0$, where $\theta_0 \approx 74°$. In Fig. 4, the curves $W_{n,T2}(\theta)$ for $n = 1, \ldots, 17$ are compared to the n-independent contribution of the term $W^{(1)}_{T2}(\theta)$, which according to (8) bears the sign of the curvature $\kappa_{T2}(\theta)$ ($\lessgtr 0$ for $\theta \lessgtr \theta_0$) of $S_{T2}(\theta)$. It is seen that the dispersion coefficients $W_{n,T2}(\theta)$ for the higher-order branches tend to approximately follow the trend of angular dependence of $W^{(1)}_{T2}(\theta)$.

Now we will examine closer the impact of tangent in the interference term

$$W^{(2)}_{n,\alpha} \sim \frac{1}{n} \sum_{\beta=1,\beta\neq\alpha}^{3} \tan\left[\frac{\pi n}{2}\left(1 - \frac{c_\alpha}{c_\beta}\right)\right], \tag{15}$$

see Eq. (9). Occasionally large absolute values of this tangent for certain branches n of the αth family perturb the convergence of $W_{n,\alpha}$ to a constant $W^{(1)}_{\alpha}$ with growing n and, moreover, may break the correspondence of signs of $W_{n,\alpha}$ and $W^{(1)}_{\alpha}$ even though n is large. Let us exemplify this aspect. Fig. 5a displays $W_{n,\alpha}(n)$ as a discrete function of integers n (the n-range is intentionally extended) and compares it to the benchmark $W^{(1)}_{\alpha}$ for the $\alpha = T2$ family of dispersion branches in a fixed sagittal plane $(\mathbf{m},\mathbf{n})$ of the (100)-cut TiO_2 plate. Because the polarization vector $\mathbf{a}_{T1}$ of the $T1$ wave makes rather a small angle $\theta = 20°$ with $(\mathbf{m},\mathbf{n})$, i.e. $\mathbf{a}_{T1}$ is not far from the SH-polarization, a coupling of the $T2$ modes to the L modes is markedly stronger than to $T1$. Hence a discrete set of values $W_{n,T2}(n)$ approximately lies on a 'n^{-1} times tangent' discontinuous curve, given by a single term of (15) with $c_\alpha/c_\beta = c_{T2}/c_L \approx 0.84$ and shifted by $W^{(1)}_{T2} < 0$. It is a relatively steady (in the measure of proximity of $|c_{T2}/c_L|$ to *1*) and increasing in n (due to $c_{T2}/c_L < 1$) curve, which gradually holds down to $W^{(1)}_{T2}$ with growing n except for the asymptotes near poles repeated with a period $P = 2/|1 - c_\alpha/c_\beta| \approx 12.7$. Note that, by (8) and (9), $W^{(1)}_{\alpha}/W^{(2)}_{n,\alpha}$ contains a factor $(1 - c^2_\alpha/c^2_\beta)$ which is rather small for the case in hand, that is why the coefficient $W_{n,T2} = W^{(1)}_{T2} + W^{(2)}_{n,T2}$ with $W^{(1)}_{T2} < 0$ and $W^{(2)}_{n,T2}(\sim n^{-1}) > 0$ is positive in the first half-period

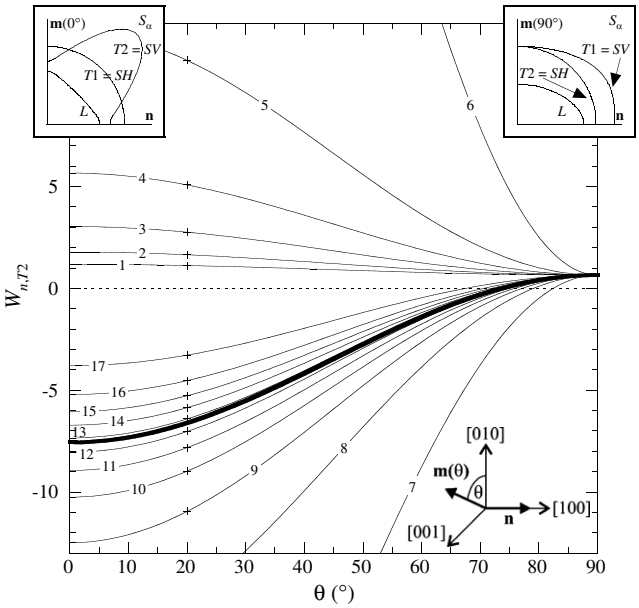

Fig. 4. The leading-order dispersion coefficient $W_{n,T2}(\theta)$ (thinner lines numbered by n) and its 'curvature-related' part $W^{(1)}_{T2}(\theta)$ (bold line) for the $\alpha = T2$ family of branches $\omega_{n,T2}(k)$ in the (100)-cut TiO_2 plate as functions of the angular orientation of the sagittal plane turning from $\theta = 0°$ to $\theta = 90°$ about the normal $\mathbf{n}\|[100]$. The lower inset explains the geometry, the upper insets display the slowness-surface cuts by the sagittal plane at $\theta = 0°$ and $\theta = 90°$. The values $W_{n,T2}$ for $\theta = 20°$ labeled by crosses appear also in Fig. 5a.

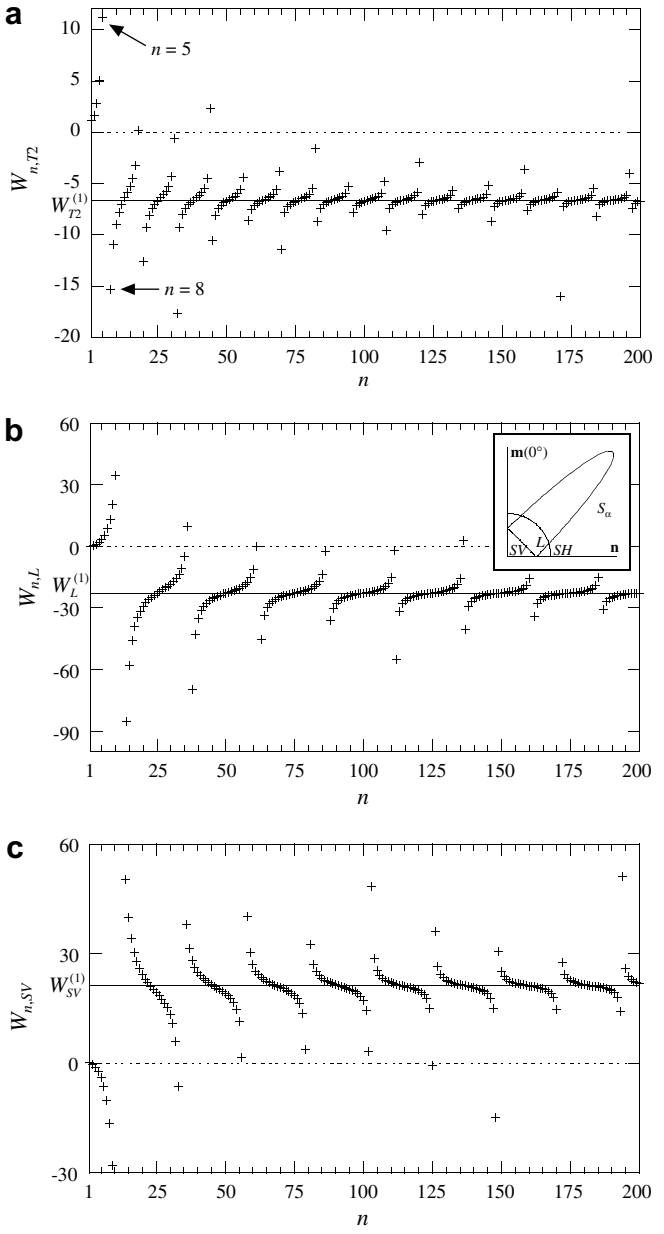

Fig. 5. The coefficient $W_{n,\alpha}$ (crosses) as a function of n (a) for the $\alpha = T2$ family of dispersion branches in the $\theta = 20°$ sagittal plane of the (100)-cut TiO_2 plate (see Figs. 2 and 3); (b) for the $\alpha = L$ and (c) for the $\alpha = SV$ family of branches in the (001) sagittal plane of the (100)-cut TeO_2 plate. The horizontal benchmark is the 'curvature-related' contribution $W^{(1)}_{\alpha}$. The inset to (b) depicts the bulk-wave slowness curves of TeO_2 in the sagittal plane.

$n \leqslant 6 < P/2$ and so the first six branches $\omega_{n,T2}(k)$ in Fig. 3 bend upwards. With growing $n > 6$, the values $W_{n,T2}$ tend to group around the 'curvature-related' contribution $W^{(1)}_{T2} < 0$ except for some secluded n, for which large $|W_{n,T2}|$ fall out on the quasi-tangent asymptotes. Such are for instance the values $W_{n,T2}$ for the branches $n = 6,7$ which exceed the vertical bounds and are therefore missing in Fig. 5a (cf. Figs. 2 and 3). As a matter of fact, an extremely large $|W_{n,\alpha}|$ signals that the quadratic-dispersion approximation (3) as a whole is no good and should be replaced by the quasilinear-dispersion fit discussed below in Section 6.

Fig. 5b presents a similar diagram for the family of dispersion branches originating from the resonances of the $\alpha = L$ longitudinal wave in the (001) symmetry plane of the (100)-cut plate of tellurium dioxide (TeO_2, the

material constants are taken from Auld (1973)). The slowness curve S_L has a prominent concavity around the plate normal $\mathbf{n}\|[100]$ (see the inset) which leads to a large absolute value of $W_L^{(1)} < 0$. The near-cutoff coefficient $W_{n,L}$ is given by Eq. $(13)_3$ where $c_{33} < c_{55}$ ($X_3\|\mathbf{n}$). Fig. 5b reveals a quasi-tangent envelope, which is determined by single-termed (15) with $c_\alpha/c_\beta = c_L/c_{SV} \approx 0.92$ and is shifted by $W_L^{(1)}$. After its first pole at $P/2 \approx 12.4$ that is for $n > 12$, the coefficient $W_{n,L}$ becomes negative and stays as such except for some of the extreme values on the quasi-tangent asymptotes.

It is thus confirmed that a local concavity of the slowness curve S_α of the resonant αth bulk mode leads to the systematic occurrence of downward onset for the high-order dispersion branches $\omega_{n,\alpha}(k)$ once their number n exceeds a certain threshold value, above which there is only a sparse sequence of upward-bending branches persisting until probably very large n. On the same grounds, a convexity of S_α makes the existence of the backward Lamb waves increasingly improbable for the high-order branches $\omega_{n,\alpha}(k)$.

In conclusion, it is interesting to note an approximately mutually exclusive fashion in which the backward Lamb waves may come about near the resonances of bulk waves with a (locally) concave and convex slowness curves. This reciprocity is nearly exact for a type of plate configurations exemplified in Figs. 2–4 where a concavity of the intermediate slowness curve comes close to the innermost slowness curve in the sagittal plane $(\mathbf{m},\mathbf{n})$ parallel (or close) to a symmetry plane. In other words, this is the case when the two in-plane (or quasi-in-plane) bulk waves have close velocities $c_\alpha/c_\beta \sim 1$ and close absolute values of slowness curvatures with opposite signs. Hence the above analysis of Fig. 5a and b, which has been developed for the resonant αth wave with a concave S_α ($\alpha = T2$ for TiO_2 and $\alpha = L$ for TeO_2), can be repeated for the resonant αth wave taken on the innermost convex S_α ($\alpha = L$ for TiO_2 and $\alpha = SV$ for TeO_2) with the only difference that the governing velocity ratio c_α/c_β is now close to 1 from above. Basically it means that the 'quasi-tangent' envelope appearing in Fig. 5a and b should be mirror-reflected about the horizontal axis. This explains why in the TiO_2-plate spectrum shown in Fig. 3 (S_{T2} is concave, S_L is convex) the first six downgoing branches of the $T2$ family are accompanied by exactly six upgoing of the L family and vice versa for higher-order $T2$ and L branches. A similar mutually exclusive reciprocity of the TeO_2-plate branches associated with a concave and a convex slowness curve can be observed on comparing Fig. 5b and c.

4.2. Sufficient condition for non-existence of backward Lamb waves near the resonances associated with a convex slowness curve

Consider the resonances of an αth bulk wave, whose slowness curve S_α in the sagittal plane $(\mathbf{m},\mathbf{n})$ is convex around $\mathbf{n}$. Note that this is always so if the αth bulk wave is the fastest along $\mathbf{n}$. The convexity of S_α ensures that $W_\alpha^{(1)} > 0$ and so the dispersion coefficient $W_{n,\alpha} = W_\alpha^{(1)} + W_{n,\alpha}^{(2)}$ is assuredly positive if $W_{n,\alpha}^{(2)} \geqslant 0$. By virtue of (9), the latter is the case when

$$\tan\left[\frac{\pi n}{2}\left(1 - \frac{c_\alpha}{c_\beta}\right)\right] \geqslant 0 \quad \text{for } \beta = 1,2,3 \neq \alpha. \tag{16}$$

Thus, once the plate normal $\mathbf{n}$ is chosen within the range of convexity of a slowness curve S_α in a cut by some plane, then the inequality (16) provides a sufficient condition that the dispersion branch, originating in this cut plane from the nth resonance of the αth bulk wave, has a positive dispersion coefficient $W_{n,\alpha} > 0$ at the onset. Note that the above derivation is based on Eqs. (7)–(9), for which the resonant αth wave is assumed non-degenerate unless the sagittal plane $(\mathbf{m},\mathbf{n})$ is a symmetry plane and hence a degeneracy $c_\alpha = c_\beta$ involves an uncoupled SH wave.

5. Dispersion near resonances of degenerate waves in the case of a non-symmetric sagittal plane

Suppose that the plate normal $\mathbf{n}$ is an acoustic axis, i.e. two of three bulk waves travelling along $\mathbf{n}$ have the same velocity, and that the sagittal plane $(\mathbf{m},\mathbf{n})$ is not a symmetry plane. This may be the case for a cubic, tetragonal or trigonal plate, which is cut orthogonally to the fourfold or threefold symmetry axis. Given so, Eqs. (7)–(9) still hold for the dispersion coefficient $W_{n,L}$ of the branches originating at the longitudinal-wave resonances (see Section 3.2). At the same time, these equations are no longer valid for the branches which emerge pairwise from resonances of degenerate transverse waves.

5.1. Normal to the plate is the fourfold axis

Consider first a tetragonal or cubic plate with **n** parallel to the fourfold symmetry axis. Assume the same setting of the coordinate axes as for (13), that is, $X_{1,2}\|\mathbf{e}_{1,2}$ (both orthogonal to the symmetry planes) and $X_3\|\mathbf{n}$. Near the degenerate transverse cutoffs $\Omega_{n,T}=\pi n c_T/d$ ($c_T=\sqrt{c_{44}/\rho}$), the dispersion coefficient as a function of the orientation θ of the sagittal plane (**m**,**n**) with **m**(θ) turning about **n** is given by

$$W_{n,\alpha}(\theta)=f+\chi_n\mp\sqrt{g^2\cos^2 2\theta+h^2\sin^2 2\theta+2\chi_n(g\cos^2 2\theta+h\sin^2 2\theta)+\chi_n^2}, \tag{17}$$

where $\alpha=T1$, $T2$ implies a pair of branches starting at $\Omega_{n,T}$, and the following notations are used

$$\begin{aligned} f&=\frac{1}{2c_{44}}\left[c_{11}+c_{66}-\frac{(c_{13}+c_{44})^2}{c_{33}-c_{44}}\right],\quad g=f-\frac{c_{66}}{c_{44}},\quad h=f-\frac{c_{11}-c_{12}}{2c_{44}};\\ \chi_n&=\frac{2}{\pi n}\sqrt{\frac{c_{44}}{c_{33}}}\left(\frac{c_{13}+c_{33}}{c_{33}-c_{44}}\right)^2\tan\left[\frac{\pi n}{2}\left(1-\frac{c_T}{c_L}\right)\right]. \end{aligned} \tag{18}$$

The radicand in (17) is indeed non-negative. Note that $g=h$ implies transverse isotropy about **n**. Also note that $f>g,h$, hence $W_{n,\alpha}(\theta)$ is assuredly positive for both if simultaneously $f\geqslant 0$ and $\tan\left[\frac{\pi n}{2}(1-\frac{c_T}{c_L})\right]\geqslant 0$. Let the labels $\alpha=T1,T2$ in (17) correspond to the upper and lower signs on the r.h.s., respectively, so that $\omega_{n,T1}(k)<\omega_{n,T2}(k)$ for a fixed non-zero $kd\ll 1$. This choice can be shown to be in one-to-one correspondence with labelling the outer and inner slowness curves of the quasi-transverse bulk modes near their degeneracy as, respectively, $S_{T1}(\theta)$ and $S_{T2}(\theta)$.

Eq. (17) reduces to the *SH*/in-plane uncoupled Eqs. $(13)_{1,2}$ in the principal symmetry plane ($\theta=\frac{\pi m}{2}$) or to their analogue in the diagonal symmetry plane ($\theta=\frac{\pi}{4}+\frac{\pi m}{2}$). Otherwise, for a general orientation of the sagittal plane (**m**, **n**), the structure of Eq. (17) is essentially different from that of Eq. (7), in which no degeneracy is involved. At the same time, if the interference parameter $|\chi_n|\sim n^{-1}$ becomes small due to n being large enough and not incidentally close to a pole of tangent in (18), then Eq. (17) admits an asymptotic form

$$W_{n,\alpha}(\theta)\approx W_\alpha^{(1)}(\theta)+\widetilde{W}_{n,\alpha}^{(2)}(\theta)\ \text{for}\ n\gg 1,\quad \alpha=T1,T2. \tag{19}$$

It is similar to (7) in that $\widetilde{W}_{n,\alpha}^{(2)}(\theta)\sim n^{-1}\tan\left[\frac{\pi n}{2}(1-\frac{c_T}{c_L})\right]$ while $W_\alpha^{(1)}(\theta)$ is independent from n. Moreover, $W_\alpha^{(1)}(\theta)$ is defined by the local shape of the bulk-wave slowness curve $S_\alpha(\theta)$ in the cuts by the sagittal plane in exactly the same way as in $(8)_1$ (with $\cos\psi_\alpha=1$ due to the fourfold symmetry of **n**). That is, $W_\alpha^{(1)}(\theta)$ in (19) is

$$W_\alpha^{(1)}(\theta)=c_T\kappa_\alpha(\theta)=f\mp\sqrt{g^2\cos^2 2\theta+h^2\sin^2 2\theta},\quad \alpha=T1,T2, \tag{20}$$

where we have used the expression of Shuvalov and Every (1996)[2] for the curvatures $\kappa_\alpha(\theta)$ of the curves $S_\alpha(\theta)$ at their touching point on the fourfold symmetry axis. Like in (17), the upper and lower signs in (20) correspond, respectively, to the outer and inner slowness curves $S_{T1}(\theta)$ and $S_{T2}(\theta)$. The curvature $\kappa_{T2}(\theta)$ is always positive for any θ, i.e. the inner curve $S_{T2}(\theta)$ is always convex ($\kappa_{T2}(\theta)>0$ for any θ). The $\kappa_{T1}(\theta)$ of the outer curve $S_{T1}(\theta)$ is positive for any θ if $g,h>-f$, negative for any θ if $g,h<-f$, and it changes sign four times with θ sweeping 180° if $(-f)$ falls in between g and h (Shuvalov and Every, 1996).

As an example, we take the (001)-cut cubic plate of gallium arsenide (GaAs, the material constants are taken from Auld (1973)). Fig. 6a shows the dispersion spectrum $\omega_{n,\alpha}(k)$ in a non-symmetric sagittal plane (**m**, **n**), for which the pairs of branches starting at the resonances of degenerate transverse waves are approximated by means of Eq. (3) with the leading-order coefficient $W_{n,\alpha}$ given by Eq. (17). The outer slowness curve S_{T1} is concave around $\mathbf{n}\|[001]$ hence the displayed branches $\omega_{n,T1}(k)$ have a downward-bending onset once $n>3$, except for the $n=10$ branch. The axial concavity of the curves $S_{T1}(\theta)$ persists for any orientation θ

[2] See Eq. (45) in Shuvalov and Every (1996), where the notations f, g, h differ from (18) by a common factor $2c_{44}$. Note a few misprints in that paper. In (1), the second sign is plus. In (26), the r.h.s. must be multiplied by $\frac{1}{2}$. The last word on the last but one line of Section III is "outmost", and on the next line the inequality sign is "<". In $(42)_1$, the second sign on the r.h.s. is minus. The first line of (57) reads "either $g>0$, or both $g<0$ and $f+g>2h^2/g$", and the second line reads likewise. On the 13th line of the last page, the reference is to (37), not (30).

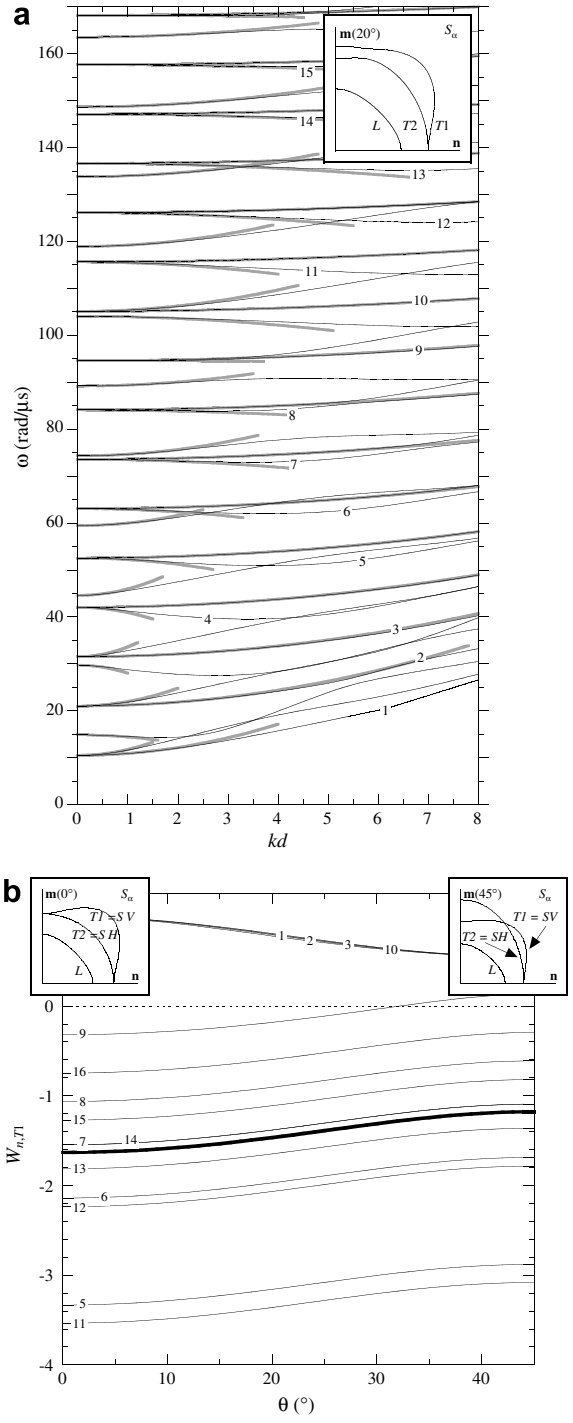

Fig. 6. The (001)-cut GaAs plate: (a) the onset of non-fundamental dispersion branches $\omega_{n,\alpha}(k)$ (solid lines; the numbered ones are for $\alpha = T1$) and their leading-order approximation (gray lines) in a non-symmetric sagittal plane $(\mathbf{m},\mathbf{n})$, which makes the angle $\theta = 20°$ with the [100]-axis; (b) the dispersion coefficient $W_{n,T1}(\theta)$ (thinner lines numbered by n; the upper ones nearly merge) and the asymptotic 'curvature-related' term $W^{(1)}_{T1}(\theta)$ (bold line) as a function of the angular orientation θ of $(\mathbf{m},\mathbf{n})$. The insets show the bulk-wave slowness curves in $(\mathbf{m},\mathbf{n})$.

of the sagittal plane in a symmetry irreducible sector $0 \leqslant \theta \leqslant 45°$. Fig. 6b relates the angular dependence of the dispersion coefficients $W_{n,T1}(\theta)$ to that of the 'curvature-related' asymptotic term $W^{(1)}_{T1}(\theta)$ defined by Eq. (20). This diagram confirms that, despite a different form of Eq. (17) comparatively to Eq. (7), there is the same link as in the general case (not involving degeneracy) between the systematic occurrence of backward Lamb waves at the onset of high-order branches and the concavity of bulk-wave slowness curve.

5.2. Normal to the plate is the threefold axis

Similar conclusions hold for a plate with the normal **n** parallel to the threefold symmetry axis. Consider a trigonal plate and introduce the coordinate axes so that the threefold axis is $X_3 \| \mathbf{n}$ and $c_{25} = 0$, $c_{14} > 0$. The coefficients $W_{n,\alpha}(\theta)$ near the degenerate transverse-wave resonances are

$$W_{n,\alpha}(\theta) = f - \frac{c_{14}^2}{c_{44}^2} + \chi_n \mp \sqrt{g^2 \sin^2 3\theta + 2g\chi_n \sin 3\theta + \chi_n^2}, \quad \alpha = T1, T2. \tag{21}$$

The asymptotic form for large n is given by Eq. (19) with

$$W^{(1)}_{\alpha}(\theta) = \frac{c_T \kappa_\alpha(\theta)}{\cos^3 \psi} = f - \frac{c_{14}^2}{c_{44}^2} \mp g \sin 3\theta, \quad \alpha = T1, T2, \tag{22}$$

where $\psi = \arctan(c_{14}/c_{44})$ is the angle of conical refraction, and the formula for the curvatures $\kappa_\alpha(\theta)$ of the slowness curves $S_\alpha(\theta)$ at their crossing point on the threefold symmetry axis is taken from Shuvalov and Every (1996). In Eqs. (21) and (22), the label $\alpha = T1$, $T2$ corresponds to the outer and inner curves $S_\alpha(\theta)$ and to the upper and lower signs, respectively. Both curvatures $\kappa_\alpha(\theta)$ are positive for any θ if $c_{11} - c_{14}^2/c_{44} > (c_{13} + c_{44})^2/(c_{33} - c_{44})$, otherwise each curvature changes sign three times with the angle θ sweeping 180° (Shuvalov and Every, 1996). The result for a (111)-cut cubic plate follows via a standard re-definition of c_{ijkl}.

6. Quasilinear onset of dispersion branches

6.1. Special case of a rational ratio of velocities

The foregoing considerations have dealt with the near-cutoff dispersion $\omega_{n,\alpha}(k)$ which is quadratic in k^2 according to (3). It is however evident that the coefficient $W_{n,\alpha}$ of quadratic dispersion may turn infinite if the interference term $W^{(2)}_{n,\alpha}$ given by (9) (see also (18)) contains an infinite tangent $\tan\left[\frac{\pi n}{2}\left(1 - \frac{c_\alpha}{c_\beta}\right)\right]$ multiplied by a non-zero prefactor. The latter is the case provided that $\|\mathbf{mn}\|_{\alpha\beta}$ and/or $\|\mathbf{mn}\|_{\beta\alpha}$ does not vanish, which simply means that the α and β modes are coupled in a given sagittal plane $(\mathbf{m}, \mathbf{n})$ (i.e. none of them is the *SH* mode when $(\mathbf{m}, \mathbf{n})$ is symmetric). In turn, the tangent may become infinite if the velocity ratio c_α/c_β is an (irreducible) rational fraction of natural numbers M,N one of which is odd and the other even, i.e.

$$c_\alpha/c_\beta = M/N \text{ with } M, N \text{ of different parity, having no common divisors } (\neq 1). \tag{23}$$

Given so, then by (1) each cutoff $\Omega_{n,\alpha}$ of the order $n = pN$ for the αth bulk mode coincides with the cutoff $\Omega_{m,\beta}$ of the order $m = pM$ for the βth bulk mode, thus producing a degenerate resonance with the frequency

$$\Omega_p^{(d)} = \left(\frac{\pi n c_\alpha}{d}\right)_{n=pN} = \left(\frac{\pi m c_\beta}{d}\right)_{m=pM}, \quad p = 1, 2, \ldots \tag{24}$$

For these degenerate resonances, the tangent in question is zero for even p and infinite for odd p. A resulting divergence of the coefficient $W_{n,\alpha}$ signals that the underlying Eq. (3) is invalid, i.e. the leading-order dispersion is no longer quadratic in k. Regarding this case for an isotropic plate, Mindlin (1955, 1960) has shown that Eq. (3) must be replaced by an expansion with the leading-order dispersion term linear in k

$$\omega(k, \theta) = \Omega_p^{(d)} \mp \left(\frac{\partial \omega}{\partial k}\right)_{k=0} k + \cdots, \tag{25}$$

where the indices for ω are omitted for brevity. The coefficient in (25) has been established for isotropic plates by Mindlin (1955, 1960) and for a propagation direction $\mathbf{m}$ orthogonal to a symmetry plane by Kaul and Mindlin (1962a,b). The case of an isotropic plate with $c_T/c_L = 1/2$ has been recently re-visited by Werby and Überall (2002). In fact, Eq. (25) applies to an arbitrary anisotropic plate near the degenerate resonances (24) once the α and β modes are coupled, M and N are of different parity, and p is odd. Unless further specialized case of triple-degenerate resonances in a non-symmetric sagittal plane, a general form the coefficient in (25) is

$$\left(\frac{\partial\omega}{\partial k}\right)_{k=0} = \frac{2}{\Omega_p^{(d)} d}\,\frac{c_\alpha^2\|\mathbf{mn}\|_{\alpha\beta} + c_\beta^2\|\mathbf{mn}\|_{\beta\alpha}}{c_\alpha^2 - c_\beta^2}. \tag{26}$$

6.2. Quasilinear near-cutoff dispersion for real materials

Certainly a velocity ratio can never be precisely a rational fraction and so Eqs. (7)–(9) can never be valid in the exact sense. At the same time, they may hold approximately thus leading to a sequence of pairs of closely situated resonances. Given that the resonant waves are not *SH*-polarized, each pair with odd p gives rise to a pair of dispersion branches starting up with a strong quadratic dependence on k (large coefficient $|W_{n,\alpha}(n)|$ due a large tangent in the interference term $W_{n,\alpha}^{(2)}$) but then they rapidly (i.e. for yet small kd) switch to the quasilinear dependence on k. The latter can be approximated by Eqs. (25) and (26). It is essential that these branches must have mutually inverse slopes, i.e. one of them slopes downwards and hence yields the backward Lamb waves. In this case they occur regardless of a local shape of the bulk-wave slowness surface, so that the upward and downward branches may correspond to the resonant modes with a concave and convex slowness curves, respectively (or to both ones convex). Thus an occasional violation of the one-to-one correspondence between the curvature of bulk-wave slowness curves and the near-cutoff trend of high-order Lamb branches discussed in Section 4.1 is associated with closely situated pairs of resonances and break-down of a quadratic dispersion.

Closely situated resonances of different bulk modes occur in any real material. What is actually significant is that they come out as a (finite) regular sequence with a not too large step provided that the velocity ratio c_α/c_β of two bulk waves, none of which is the *SH* mode, is close enough to a rational fraction M/N with M and N being relatively small integers of different parity. For example, in the case of TiO_2-plate shown in Fig. 3, the ratio c_{T2}/c_L lies in between 5/6 and 6/7. That is why the branches emerging from the nearly situated cutoffs $\Omega_{5,L} \approx \Omega_{6,T2}$ and $\Omega_{7,T2} \approx \Omega_{6,L}$ have a quasilinear slope of an opposite sign. It is approximated in Fig. 3 (dashed lines) by Eqs. (25) and (26) with $\Omega_1^{(d)}$ ($p = 1$) taken as a 'fictitious' degenerate cutoff equidistant from the actual neighbouring $T2$ and L cutoffs. As noted below (24), an even $p = 2$ nullifies the tangent factor in the corresponding interference parameter, and hence the next pairs of close resonances of $T2$ and L waves in Fig. 3 ($n = 12, 13$ for $T2$ and *10,11* for L) give rise to the branches which are well fitted by the quadratic-dispersion approximation with a coefficient determined mainly by the 'curvature-related' contribution. The latter aspect is visualized in Fig. 4, where the curves $W_{n,T2}(\theta)$ for $n = 12, 13$ are quite close to the curve $W_{T2}^{(1)}(\theta)$ for the full angular range. The next occasion of proximity of $T2$ and L resonances, corresponding to (24) with $p = 3$ ($n = 19$ for $T2$ and 16 for L, not shown in Figs. 2–4), again brings about a pair of branches with quasilinear onset. In Fig. 3, the polarization of $T1$ bulk wave has rather a small $\theta = 20°$ deviation from the *SH*-polarization, hence a proximity of its resonances to the resonances of L and $T2$ waves is of minor significance. It is however demonstrated that the close resonances $\Omega_{2,L} \approx \Omega_{3,T1}$ produce a quasilinear dispersion approximated in Fig. 3 by Eqs. (25) and (26).

As another example, we consider the (001)-cut cubic copper plate (the material constants $c_{11} = 169$, $c_{12} = 122$, $c_{44} = 75.3$ GPa and $\rho = 8.932$ g/cm^3 are taken from Every and McCurdy (1992)). This case is interesting for it yields the ratio c_T/c_L which is extremely close (from above) to 2/3. The dispersion spectrum for in-plane Lamb waves in the (100)-sagittal plane is shown in Fig. 7a (the *SH* branches are omitted). The quadratic-dispersion approximation is given by Eq. $(13)_{2,3}$. It fits the onset of all the detached branches and also of the two branches emerging from the second pair of nearly degenerate L and SV resonances (even $p = 2$ in (24)), but it breaks away very rapidly from the branches starting at the first and third pair of such resonances (odd $p = 1, 3$). These latter branches are well fitted by the linear-dispersion approximation given by Eqs. (25) and (26).

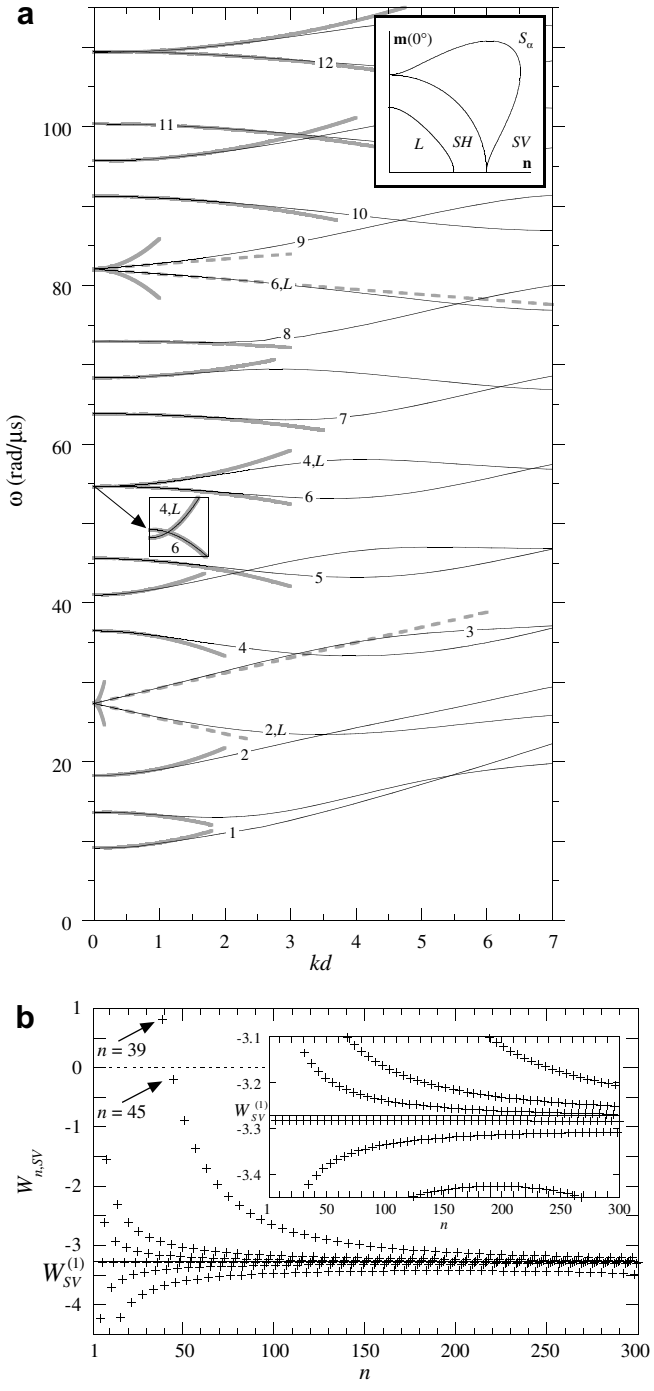

Fig. 7. The (100) sagittal plane (**m**, **n**) in the (001) cut copper plate: (a) the onset of the in-plane non-fundamental dispersion branches $\omega_{n,\alpha}(k)$ (solid lines; the numbered ones are for $\alpha = SV$) along with their leading-order quadratic (gray lines) and quasilinear (dashed lines) approximation; (b) the coefficient $W_{n,T1}$ as a discrete function of n (crosses) compared to the 'curvature-related' term $W_{T1}^{(1)}$. The inset to (a) shows the bulk-wave slowness curves in the sagittal plane. The inset to (b) zooms on the values of $W_{n,T1}$ in the vicinity of $W_{T1}^{(1)}$, which is indicated by the horizontal line.

Staying with the example of the copper plate enables us to highlight some other subtle aspects of the dispersion near quasi-degenerate resonances. According to the preceding analysis, a concavity of the slowness curve S_{SV} (see inset to Fig. 7a) leads to the downward onset of high-order dispersion branches $\omega_{n,SV}(k)$ once

$n > 3$ and except for the branch numbers $n = 3p$ with odd p, when the cutoffs $\Omega_{3p,SV}$ come close (from above) to the cutoffs $\Omega_{2p,L}$ (which in turn give rise to the exceptional downward-bending branches of the L-family). By virtue of $c_T/c_L = (2/3) + \varepsilon$ where $0 < \varepsilon \ll 1$, the quadratic-dispersion coefficient $W_{n,SV}(n)$ as a discrete function of n is proportional to

$$n^{-1} \tan\left(\frac{\pi n}{6} - \frac{\pi}{2} n\varepsilon\right) \tag{27}$$

with a shift by $W_{SV}^{(1)} < 0$. The values $W_{n,SV}(n)$ shown in Fig. 7b are distributed along these tangent curves in a way which sets apart six subsets: one, for $n = 3p$ with even p, lies on a straight-like line and five others are placed along hyperbola-like lines (note a striking difference from Fig. 5). The upper hyperbola, for $n = 3p$ with odd p, traces the values $W_{n,SV}(n)$ falling out just before (due to $\varepsilon > 0$) the tangent poles. It tells us that the exceptional branches of the SV family have an upward trend until $n = 45$ (indicated in Fig. 7b), above which $n\varepsilon$ in (27) is no longer small enough. Attention is drawn to the fact that a strong quadratic-dispersion dependence due to a large tangent is in fact rapidly replaced by a smoother quasilinear dispersion, but we can be sure that both of them have the same sign for a given branch. In other words, the exceptional branches $\omega_{n,SV}(k)$ for $n = 3p < 45$ with odd p retain upward trend when passing from the quadratic-dispersion onto the adjacent quasilinear range, and correspondingly $\omega_{m,L}(k)$ for $m = 2p < \ldots$ with odd p remain being downward. Indeed otherwise would cause crossing of these $\omega_{n,SV}$ and $\omega_{m,L}$ branches which is impossible as they are either both symmetric or both antisymmetric due to $n = 3p$ and $m = 2p$ being of different parity when p is odd (in contrast to the case of even p, see the zoom of $\omega_{6,SV}(k)$ and $\omega_{4,L}(k)$ in Fig. 7a). To highlight this aspect, imagine for the moment a slight perturbation of c_{11} and c_{44} such that inverts the sign of $\varepsilon = c_T/c_L - (2/3)$ from positive to negative and hence inverts the neighbouring cutoffs so that now $\Omega_{2p,L} > \Omega_{3p,SV}$. Correspondingly, the upward and downward (quadratic) branches associated with even p shift with respect to each other, so that they no longer intersect. One could expect that a pair of quasilinear branches for odd p also undergo the same kind of transition through each other, but then this would lead to their intersection which is forbidden. Thus what happens in fact is that the upper, upwards going SV branch and the lower, downwards going L branch approach each other at $\varepsilon \to 0$ and meet at the degenerate cutoff when $\varepsilon = 0$, but then, for $\varepsilon < 0$, these branches move apart retaining their dispersion trends. At the same time, the upper (and upward) branch becomes the L-branch while the lower (and downward) branch becomes the SV-branch. This is in agreement with (27), according to which the upper hyperbola in Fig. 7b is mirror-reflected about the horizontal axis when ε becomes negative.

7. Conclusions

In brief summary, the coefficient of leading-order dispersion $\omega_{n,\alpha}(k) - \Omega_{n,\alpha} \sim O(k^2)$ at the onset of Lamb-wave branches (n is the branch number for the family originating at the cutoff frequency $\Omega_{n,\alpha}$ of resonances of $\alpha = 1, 2, 3$ bulk waves) has been derived for an arbitrary anisotropic plate. Its negative sign identifies a downward trend at the onset of branches $\omega_{n,\alpha}(k)$ and hence the near-cutoff existence of backward Lamb waves with a negative (in-plane) group velocity. The sign analysis is based on the observation that this coefficient contains two contributions: one is determined by the curvature of resonant bulk-wave slowness curve S_α in the sagittal plane, the other describes modal interference in a Lamb-wave packet. For a special case, when the plate normal is an acoustic axis and the sagittal plane is not a symmetry plane, the dispersion coefficient is given by a more complicated formula; however, its asymptotic form for large enough n also acquires the above-mentioned structure with two additive terms of different nature. On taking out a common factor n^{-1}, the former term is independent from n, while the latter contains an additional factor n^{-1} and is also proportional to a tangent depending on n. As result, a local concavity of the slowness curve S_α of the αth bulk wave causes a systematic occurrence of downward bent for the branches $\omega_{n,\alpha}(k)$ whose number n exceeds certain threshold n_0 (for several examples of materials considered in the paper, n_0 has ranged from 3 for GaAs and Cu to 12 for TeO_2). The high-order branches of αth family (S_α is concave) starting from the cutoff frequency $\Omega_{n,\alpha} > \pi n_0 c_\alpha / d$ admit an upward bent only occasionally, for a sparse sequence of branches which fall out with a step of about $2n_0$ in n until some large n. On the same grounds, a convex slowness curve of the resonant bulk wave entails the downward trend of the high-order branches with only rare exceptions. A

sequence of the exceptional high-order branches, for which the near-cutoff dispersion trend is irrelevant to the shape of slowness curve of the resonant bulk wave, is associated with a pairwise proximity of resonances giving rise to pairs of dispersion branches with upward and downward quasilinear onset. This feature is especially prominent and regular in a spectrum where the velocity ratio for two resonant bulk waves, none of which is the *SH* mode, is close to a fraction of relatively small integers of different parity.

In conclusion, let us cast a brief glance on the problem of backward Lamb waves in a broader sense, which is not restricted to the near-cutoff vicinity (in doing so, it is suitable to label the dispersion branches by a single index $J = 1,2,\ldots$ instead of (n,α) as elsewhere). It is evident that the approach of the present study, which is confined to the leading-order dispersion near cutoffs, is unable to give us the point where the downward onset of a dispersion branch in a given sagittal plane $(\mathbf{m},\mathbf{n})$ switches to the upward trend, i.e., where its initially negative group velocity $g_J^{(\mathbf{m})}(k)$ in a given sagittal plane $(\mathbf{m},\mathbf{n})$ turns to zero and becomes positive with further growing k. Neither it can predict occasions of negative $g_J^{(\mathbf{m})}(k)$, and hence of spectral zones of backward Lamb waves, in the intervals which are not adjacent to a cutoff. A possible existence of such intervals has been demonstrated by Solie and Auld (1973) and Li and Thompson (1990) and emphasized recently by Parygin et al. (2000) for anisotropic plates with a boundary parallel to symmetry plane (which allows intersection of dispersion branches). Alternating intervals of positive and negative $g_J^{(\mathbf{m})}(k)$ along dispersion branches occur due to their weaving shape, which is especially salient in the case of a prominent concavity of the bulk-wave slowness sheets both along $\mathbf{n}$ and along $\mathbf{m}$, like in the (100)-cut TeO_2 plate (Parygin et al., 2000). Note also that a proximity of $v_J(k)$ to the real part of velocity of the leaky wave for a halfspace consisting of the plate material $(d \to \infty)$ may be a favorable factor for the backward propagation of Lamb waves provided that the group-velocity vector of the partial bulk mode of this leaky wave has a negative projection on $\mathbf{m}$. Certainly $g_J^{(\mathbf{m})}(k) = v_J(k) + kv'_J(k)$ must become positive definite on descending down any phase-velocity branch $v_J(k)$ (or $v_J(\omega)$) since its dispersion falls off sooner or later. In this light, another intriguing question arises: what is the absolute phase-velocity bound, below which no branch $v_J(k)$ or $v_J(\omega)$ can admit negative $g_J^{(\mathbf{m})}$? Altogether, the above-mentioned issues invite further research into the backward propagation of Lamb waves in anisotropic plates.

Acknowledgements

The authors are grateful to V.G. Mozhaev and A.G. Every for the stimulating discussions. A.L.S. acknowledges partial support from the Russian Foundation for Basic Research (Grant 05-02-16666).

References

Auld, B.A., 1973. Acoustic Fields and Waves in Solids. Wiley-Interscience Publication, New York.

Balogun, O., Murray, T.W., Prada, C., 2007. Simulation and measurement of the optical excitation of the S_1 zero group velocity Lamb wave resonance in plates. Journal of Applied Physics 102, 064914.

Castaings, M., Hosten, B., 2003. Guided waves propagating in sandwich structures made of anisotropic, viscoelastic composite materials. Journal of the Acoustical Society of America 113, 2622–2634.

Clorennec, D., Prada, C., Royer, D., Murray, T., 2006. Laser impulse generation and interferometer detection of zero group velocity Lamb mode resonance. Applied Physics Letters 89, 024101.

Clorennec, D., Prada, C., Royer, D., 2007. Local and nonlocal measurements of bulk acoustic wave velocities in thin isotropic plates and shells using zero group velocity Lamb modes. Journal of Applied Physics 101, 034908.

Durinck, G., Thys, W., Rembert, P., Izbicki, J.-L., 2002. Experimental data supporting calculations of the angular derivative of the phase of transmission coefficient of an elastic plate. Wave Motion 35, 271–273.

Every, A.G., McCurdy, A.K., 1992. Numerical data and fundamental relationships in science and technology. In: Nelson, D.F. (Ed.), . In: New Series, Group III of Landolt-Bernstein, vol. 29a. Springer, Berlin.

Germano, M., Alippi, A., Angelici, M., Bettucci, A., 2002. Interference between forward and backward propagating parts of a single acoustic plate mode. Physical Review E 65, 046608.

Gridin, D., Adamou, A.T.I., Craster, R.V., 2005. Trapped modes in curved elastic plates. Proceedings of the Royal Society A 461, 1181–1197.

Holland, S.D., Chimenti, D.E., 2004. High contrast air-coupled acoustic imaging with zero group velocity Lamb modes. Ultrasonics 42, 957–960.

Kaplunov, J.D., Kossovich, L.Yu., Rogerson, G.A., 2000. Direct asymptotic integration of the equations of transversely isotropic elasticity for a plate near cut-off frequency. Quarterly Journal of Mechanics and Applied Mathematics 53, 323–341.

Kaplunov, J.D., Rogerson, G.A., Tovstik, P.E., 2005. Localized vibration in elastic structures with slowly varying thickness. Quarterly Journal of Mechanics and Applied Mathematics 58, 645–664.

Kaul, R.K., Mindlin, R.D., 1962a. Vibrations of an infinite monoclinic crystal plate at high frequencies and long wavelengths. Journal of the Acoustical Society of America 34, 1895–1901.

Kaul, R.K., Mindlin, R.D., 1962b. Frequency spectrum of a monoclinic crystal plate. Journal of the Acoustical Society of America 34, 1902–1910.

Li, Y., Thompson, R.B., 1990. Influence of anisotropy on the dispersion characteristics of guided ultrasonic plate modes. Journal of the Acoustical Society of America 87, 1911–1931.

Liu, T., Kaunasena, W., Kitipornchai, S., Veidt, M., 2000. The influence of backward wave transmission on quantitative ultrasonic evaluation using Lamb wave propagation. Journal of the Acoustical Society of America 107, 306–314.

Marston, P.L., 2003. Negative group velocity Lamb waves on plates and applications to the scattering of sound by shells. Journal of the Acoustical Society of America 113, 2659–2662.

Mindlin, R.D., 1955. An Introduction to the Mathematical Theory of Vibrations of Elastic Plates. Signal Corps Engineering Laboratories, Fort Monmouth, New Jersey.

Mindlin, R.D., 1960. Waves and vibrations in isotropic, elastic plates. In: Goodier, J.N., Hoff, N. (Eds.), Structural Mechanics. Pergamon, New York, pp. 199–232.

Pagneux, V., Maurel, A., 2002. Lamb wave propagation in inhomogeneous elastic waveguides. Proceedings of the Royal Society 458, 1913–1930.

Parygin, V.N., Vershoubskiy, A.V., Mozhaev, V.G., Weihnacht, M., 2000. Prolonged acousto-optic interaction with Lamb waves in crystalline plates. Ultrasonics 35, 594–597.

Pavlakovic, B.N., Lowe, M.J.S., Alleyne, D.N., Cawley, P., 1997. Disperse: a general purpose program for creating dispersion curves. In: Thompson, D.O., Chimenti, D.E. (Eds.), . In: Review of Progress in Quantitative NDE, vol. 16. Plenum Press, New York, pp. 185–192.

Pichugin, A.V., Rogerson, G.A., 2001. A two-dimensional model for extensional motion of a pre-stressed incompressible elastic layer near cut-off frequencies. IMA Journal of Applied Mathematics 66, 357–385.

Pichugin, A.V., Rogerson, G.A., 2002. Anti-symmetric motion of a pre-stressed incompressible elastic layer near shear resonance. Journal of Engineering Mathematics 42, 181–202.

Postnova, J., Craster, R.V., 2007. Trapped modes in topographically varying elastic waveguides. Wave Motion 44, 205–221.

Shuvalov, A.L., Every, A.G., 1996. Curvature of acoustic slowness surface of anisotropic solids near symmetry axes. Physical Review B 53, 14906–14916.

Shuvalov, A.L., Poncelet, O., Deschamps, M., 2006. Analysis of the dispersion spectrum of fluid-loaded anisotropic plates: leaky wave branches. Journal of Sound and Vibration 296, 494–515.

Skelton, E.A., Adams, S.D.M., Craster, R.V., 2007. Guided elastic waves and perfectly matched layers. Wave Motion 44, 573–592.

Solie, L.P., Auld, B.A., 1973. Elastic waves in free anisotropic plates. Journal of the Acoustical Society of America 54, 50–65.

Tolstoy, I., Usdin, E., 1957. Wave propagation in elastic plates: low and high mode dispersion. Journal of the Acoustical Society of America 29, 37–42.

Werby, M.F., Überall, H., 2002. The analysis and interpretation of some special properties of higher order symmetric Lamb waves: The case for plates. Journal of the Acoustical Society of America 111, 2686–2691.